

Evidence for instability in charge ordering $\text{Nd}_{0.5}\text{Sr}_{0.5}\text{MnO}_3$

Jiyu Fan^{a,*}, Yue Ying^b, Li Pi^b, Yuheng Zhang^b

^a Department of Physics, Sejong University, Seoul, 143-747, Republic of Korea

^b Hefei High Magnetic Field Laboratory, University of Science and Technology of China, Hefei 230026, People's Republic of China

Received 1 October 2006; accepted 7 October 2006 by A.H. MacDonald

Available online 23 October 2006

Abstract

The transport properties and magnetic phase transitions of charge ordering manganites $\text{Nd}_{0.5}\text{Sr}_{0.5}\text{MnO}_3$ have been investigated. From resistivity measurements, a continuous increase of resistivity upon the thermal cycling occurs at $T \leq 150$ K, and shows an instable behavior in the system. The experimental results of magnetization and electron-spin-resonance spectra indicate that the ferromagnetic phase and antiferromagnetic phase coexist in a broad temperature region. We think that the origin of the instability stems from an inhomogeneous strain yielded in the ferromagnetic interface, due to the competition among different phases.

© 2006 Elsevier Ltd. All rights reserved.

PACS: 75.47.Lx; 75.60.Ej

Keywords: A. Perovskite manganites; D. Instability

1. Introduction

The hole-doped $\text{Ln}_{(1-x)}\text{A}_x\text{MnO}_3$ (Ln = trivalent rare earth, A = divalent alkaline earth) manganites have attracted significant interest in the past decade because of their rich physical properties and potential applications [1–4]. In-depth investigations show that these rich properties originate from coupling and competition among interactions involving spin, lattice, orbit, and charge degrees of freedom [5–7]. Recently, intensive attention has been paid to the investigation of charge ordering (CO) and orbital ordering (OO) systems, which is most easily observed in half-doped $x = 0.5$ manganites [8–10]. The spatial CO phase behaves as the periodic arrangement of $\text{Mn}^{3+}/\text{Mn}^{4+}$ ions. Generally, the CO formation is accompanied by an antiferromagnetic (AFM) phase transition. The ground state, therefore, was usually assigned to be CO/AFM state. By way of example, $\text{La}_{0.5}\text{Ca}_{0.5}\text{MnO}_3$ is a ferromagnet in the temperature regime $T_{\text{CO}} \leq T \leq T_{\text{C}}$ ($T_{\text{CO}} = 190$ K, $T_{\text{C}} = 230$ K), but transforms into a CO AFM insulator at temperatures below T_{CO} [11]. Similarly, $\text{Pr}_{0.5}\text{Sr}_{0.5}\text{MnO}_3$ exists in a ferromagnetic metallic state below 250 K and becomes a

CO AFM insulator at 150 K [12]. Up to now, it has been well confirmed that the CO state stems from the interplay between Coulomb repulsion, orbital ordering and Jahn–Teller distortion.

Usually, the charge ordering state can keep stably in manganites, except for the presence of some extreme exoteric perturbations. For example, Tokunaga et al. [13] found that the CO state still remained stable even under magnetic fields up to 27 T in $\text{Pr}(\text{Nd})_{0.5}\text{Ca}_{0.5}\text{MnO}_3$. However, other experimental evidences also show that the charge ordering state can be easily adjusted by only a few impurity substitutions on the Mn-sites. For the charge ordering manganites $\text{Pr}_{0.6}\text{Ca}_{0.4}\text{MnO}_3$ and $\text{La}(\text{Pr})_{0.5}\text{Ca}_{0.5}\text{MnO}_3$, the substitution of Al^{3+} , Fe^{3+} , Ga^{3+} , and Cr^{3+} for Mn^{3+} destabilizes the CO phase very effectively, and induces ferromagnetism and the insulator–metal transition at low temperatures [14–16]. Meanwhile, an unusual phenomenon, instability, has been found in the Cr-doped $\text{Pr}_{0.5}\text{Ca}_{0.5}\text{MnO}_3$ compound by Mahendiran et al. [17]. It shows transport properties depending on the material's thermal cycling history. They proposed that the increase of the elastic energy in the ferromagnetic-charge ordered interface might be the origin of the systematic instability. Similarly, Kimura et al. [18] found that there are submicrometric ferromagnetic-metallic domains and diffuse phase transitions in the Cr-doped $\text{Nd}_{0.5}\text{Ca}_{0.5}\text{MnO}_3$ system.

* Corresponding author.

E-mail address: jiyufan@ustc.edu (J. Fan).

Furthermore, the size of the FM cluster can be controlled by a magnetic field. Therefore, a strain is easily developed at the FM–AFM interface due to the competition between these two phases. The appearance of this strain inevitably influences the material's systematic behavior, and thus results in the instability. Therefore, the competition between some different phases should be the intrinsic reason for instability regardless of whether it is in the doped CO system or undoped CO system. We notice that the property in CO manganite $\text{Nd}_{0.5}\text{Sr}_{0.5}\text{MnO}_3$ is slightly different from that in other CO systems, because its ground state exhibits a coexistence of FM and CE-type AFM phases instead of a single CO-AFM ground state as in other CO systems [19]. Therefore, we suppose that the instable behavior also shows in the $\text{Nd}_{0.5}\text{Sr}_{0.5}\text{MnO}_3$ system. In this paper, we firstly reported an instable behavior in the undoped CO system based on the observation of a continuous increase of resistivity through the thermal cycling process for seven iterations. Moreover, the instable region in the resistivity curve just corresponds to the thermal hysteresis region in the magnetization curve. It indicates that the presence of an instability is related to the systematic magnetism. By the measurement of magnetization and electron-spin-resonance (ESR) spectra, the coexistence of FM phases and the CO AFM phase was discovered in low temperatures. Therefore, we propose that the intense competition during the magnetic transition from the FM phase to the AFM phase, or from the AFM phase to the FM phase, results in the presence of a strain and the existence of instable behavior in the CO system.

2. Experiment

A polycrystalline sample $\text{Nd}_{0.5}\text{Sr}_{0.5}\text{MnO}_3$ was prepared by the conventional solid-state reaction method with high pure Nd_2O_3 , SrCO_3 , and MnO_2 , as the starting materials. The mixture was preheated in air at 900 °C for 24 h. Afterwards, the powder was ground and heated at 1200 °C for 30 h. Finally, it was reground, palletized and sintered for another 40 h at 1350 °C, and was cooled down to room temperature within the furnace. The structure and phase purity of the prepared sample was checked by powder X-ray diffraction (XRD), using Cu $K\alpha$ radiation at room temperature. The XRD patterns show that the samples exhibit a single-phase orthorhombic structure. The resistivity (ρ) was measured by the standard four-probe method. The magnetization (M) measurement was performed using a Quantum Design Superconducting Quantum Interference Device under a 0.01 T magnetic field in the range of 5–300 K. The electron-spin-resonance spectra were obtained from JES-FA200 spectrometer at 9.06 GHz.

3. Results and discussion

The temperature dependence of the resistivity $\rho(T)$ curves for the $\text{Nd}_{0.5}\text{Sr}_{0.5}\text{MnO}_3$ sample is shown in Fig. 1. All thermal cycling processes are performed firstly from room temperature down to low temperature, and then back to room temperature. Such a thermal cycling process is repeated seven times. In the first one, with the decrease of temperature, the resistivity gradually increases and then slightly decreases around the

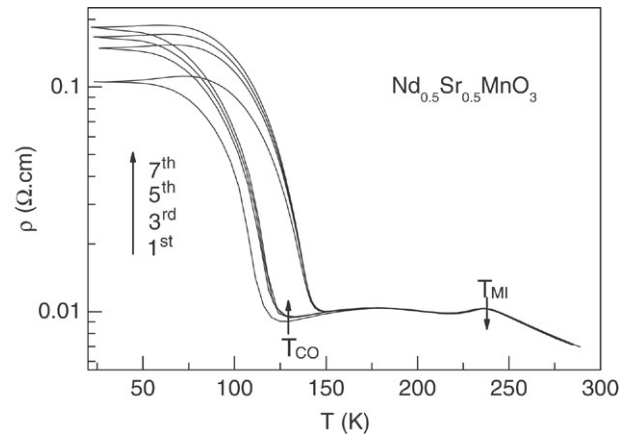


Fig. 1. Temperature dependence of resistivity for seven successive thermal cycling runs in $\text{Nd}_{0.5}\text{Sr}_{0.5}\text{MnO}_3$.

temperature $T = 240$ K. The presence of this small peak indicates the existence of an insulator–metal transition at 236 K. With the further decrease of temperature, the resistivity keeps on decreasing, but abruptly shifts to a rise near the temperature $T = 127$ K, exhibiting a change transition from a disordering state to an ordering state. Below $T = 50$ K, the resistivity almost remains unchanged. In the warming process, the variation of $\rho(T)$ curve is basically similar to that in the cooling process, except that a larger resistivity occurs in the temperature range of 50–150 K, which results in a considerable thermal hysteresis in $\rho(T)$ curve. In the subsequent thermal cycles, though the shape of $\rho(T)$ curves is similar to each other, an important variation should be clearly noticed. Below $T = 150$ K, the resistivity in the thermal hysteresis region and at the lowest temperature becomes larger and larger upon the increase of thermal cycling, similar to the behavior of the Cr-doping $\text{Pr}_{0.5}\text{Ca}_{0.5}\text{MnO}_3$ system [17]. This phenomenon has not ever been reported in $\text{Nd}_{0.5}\text{Sr}_{0.5}\text{MnO}_3$ before. Therefore, an instable behavior can also occur in the pristine charge ordering system, rather than only in the system which is substituted with impurities on Mn-sites. In the charge ordering manganites, electronic transport is strongly correlated with the magnetic transition. Therefore, we investigate its magnetic phase transition as follows.

As shown in Fig. 2, the magnetization was measured with a zero-field-cooling mode for the $\text{Nd}_{0.5}\text{Sr}_{0.5}\text{MnO}_3$ sample in the temperature range of 5–300 K. With the decrease of temperature, the magnetization starts to increase at $T = 250$ K, exhibiting a typical paramagnetic–ferromagnetic phase transition. It just corresponds to the insulator–metal transition in the $\rho(T)$ curve. At 150 K, the magnetization inclines toward saturation. However, below 150 K, the magnetization drops rapidly, and the transition is finished in a very narrow region. Here, the decrease of magnetization not only exhibits the presence of an FM–AFM phase transition, but also implies the formation of a charge ordering state. This result is in agreement with the previous ones reported by López and Kajimoto [20, 21]. At the lowest temperature, the ground state is dominated mainly by the AFM phase, but a fraction of FM phase remains in the system, as shown from the residual magnetization in

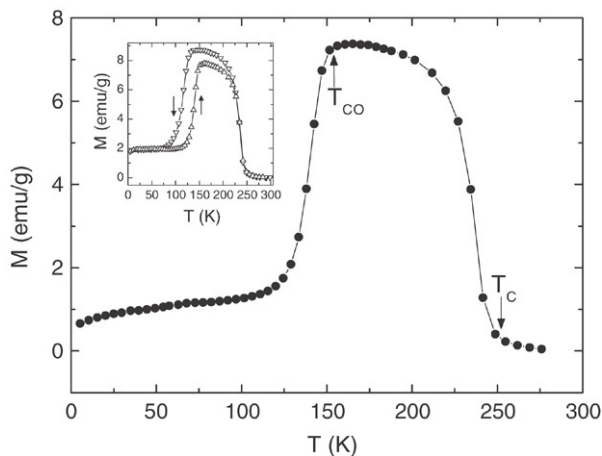


Fig. 2. Temperature dependence of the magnetization for $\text{Nd}_{0.5}\text{Sr}_{0.5}\text{MnO}_3$; the inset shows the temperature variation of the cooling magnetizations (∇) and the warming magnetizations (Δ).

the $M(T)$ curve. The inset of Fig. 2 shows the warming and cooling magnetization curve for the $\text{Nd}_{0.5}\text{Sr}_{0.5}\text{MnO}_3$ sample. In the temperature region $100 \text{ K} \leq T \leq 150 \text{ K}$, it exhibits thermal hysteresis as well. Obviously, this behavior is related to the thermal hysteresis in the $\rho(T)$ curve at the same temperature. Moreover, both the charge ordering phase and FM–AFM (AFM–FM) phase transition also occur in this temperature region. Therefore, in order to shed additional light on this phenomenon, the systematic micromagnetism has been investigated.

It is well known that ESR is highly sensitive to both minor magnetic phases and short-range interactions, and has been widely applied to research the micromagnetic properties of manganites [22–24]. Fig. 3 shows the ESR spectra for the $\text{Nd}_{0.5}\text{Sr}_{0.5}\text{MnO}_3$ sample in the temperature range 110–300 K. Clearly, there is only a single line, with a Lorentz function shape, in each spectrum from 300 K to 250 K. This signal has been referred primarily to the contribution of the PM Mn ions [25]. However, beginning from 240 K, the site of the resonance peak slowly moves to the low field region with the

decrease of temperature. Connecting this with the magnetic transition in the $M(T)$ curve, we can understand that it is due to the appearance of the FM phase. With further decreases of temperature, the FM resonance peak continually shifts to the lower field region, while its intensity starts to reduce at $T = 210 \text{ K}$. At the same time, the previous PM peak is broadened slowly, until about 150 K, when this broadened peak has become an obvious single peak. Moreover, the nascent peak shifts to the high field region, which should be attributed to the AFM resonance peak [26]. However, the FM peak still remains in the low field region. As we know, in the study of ESR spectra, the peak-to-peak width ΔH_{pp} and the resonance field H_r reflect the interaction of spins with their environment [27]. Generally, in the homogenous magnetic system, the variation of ΔH_{pp} initially linearly decreases from high temperatures to T_C , and then increases with further decreasing temperatures below T_C . Some relaxation mechanisms, such as spin–lattice relaxation and the bottlenecked spin relaxation [28,29], are used to explain the variation. Fig. 4 shows the temperature dependence of ΔH_{pp} and H_r . Obviously, their variations are opposites. In low temperatures, the rise of resonance field and the diminution of peak-to-peak width reflect the presence of magnetic inhomogeneity. Therefore, the results of ESR spectra and magnetization indicate that the current system is composed of two phases instead of a single phase. In fact, in the $M(T)$ curve, the magnetic transition has tended to become mild since $T = 200 \text{ K}$, which implies that some nano-AFM clusters have started to appear even though the CO phase transition occurs at $T = 150 \text{ K}$. Furthermore, from the ESR spectra, we can find that its intensity has been partly weakened since $T = 210 \text{ K}$. Therefore, the coexistence of the FM phase and the AFM phase is prior to the CO phase transition. With the decrease of temperature, even though the FM phase tends to reduce while the AFM phase becomes dominant, there is a small portion of FM state that survives in the AFM environment.

As noted in the introduction, Mahendiran et al. [17] found instability in the Cr-doped $\text{Pr}_{0.5}\text{Ca}_{0.5}\text{MnO}_3$ compound. Due to the substitution on Mn-sites, the long-range CO phase was separated into some short-range ones. Hence, spin

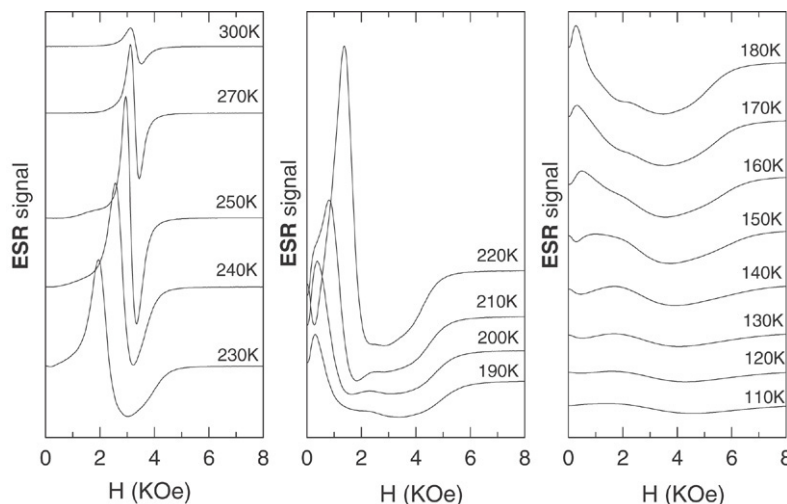


Fig. 3. Electronic spin resonance spectra of $\text{Nd}_{0.5}\text{Sr}_{0.5}\text{MnO}_3$ at different temperatures.

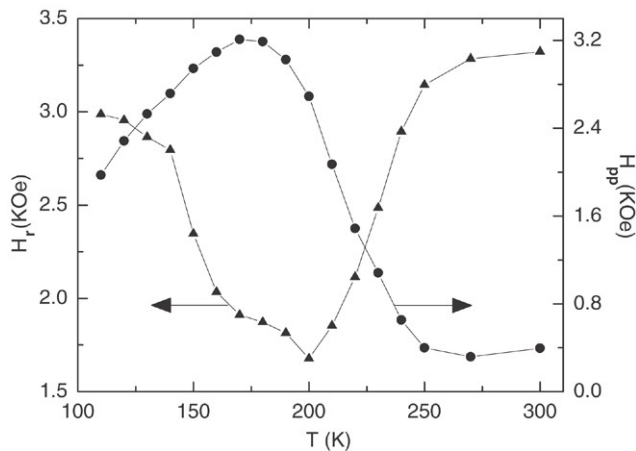


Fig. 4. The temperature variation of the peak-to-peak width ΔH_{pp} (●) and the resonance field H_r (▲) from ESR spectra.

fluctuations and metastability are introduced into the system, which weakens the magnetic coupling. Here, even though the charge/spin structure in Mn–O–Mn layer is maintained, the competition between the FM phase and the AFM phase produces the inhomogeneous strain. The inhomogeneous strain will cause some metastability, similar to the diffuse ferromagnetism noted in the Cr-doped $\text{Nd}_{0.5}\text{Ca}_{0.5}\text{MnO}_3$ system [18]. Because the FM and AFM phases coexist in the present system, the inhomogeneous strain is produced at their interface due to microstructure discrepancies between them. It inevitably influences the domain motion and the growth of the FM/AFM phases. At the end of the thermal cycling, the domain boundary is gradually changed because the accommodation strain is relaxed at the interfacial region, which not only causes the different $\rho(T)$ in every thermal cycle, but also increases the resistivity at low temperatures. Thus, resistivity instability through the thermal cycling process is observed.

4. Conclusion

In summary, the transport and magnetic properties of $\text{Nd}_{0.5}\text{Sr}_{0.5}\text{MnO}_3$ have been studied. A continuous increase of resistance through the thermal cycling process was observed, exhibiting an instable behavior in the system. The measurement of magnetization and ESR indicates that the FM phase coexists with the CO AFM phase at low temperatures. We propose that an intense competition between the FM phase and AFM phase results in the presence of a strain, which is responsible for the existence of the instable behavior in the current CO system.

Acknowledgment

This work was supported by a Korean Research Foundation Grant funded by the Korea Government (MOEHRD) (KRF-

2005-070-C00055), and by the National Nature Science Foundation of China (Grant No. 10334090 and No. 10504029).

References

- [1] R. von Helmolt, J. Wecker, B. Holzapfel, L. Schultz, K. Samwer, *Phys. Rev. Lett.* 71 (1993) 2331.
- [2] S. Jin, T.H. Tiefel, M. McCormack, R.A. Fastnacht, R. Ramesh, L.H. Chen, *Science* 264 (1994) 413.
- [3] J.M.D. Coey, M. Viret, S. von Molnar, *Adv. Phys.* 48 (1999) 167.
- [4] J.Z. Sun, W.J. Gallagher, P.R. Duncombe, L. Krusin-Elbaum, R.A. Altman, A. Gupta, Y. Lu, G.Q. Gong, G. Xiao, *Appl. Phys. Lett.* 69 (1996) 3266.
- [5] S. Mori, C.H. Chen, S.-W. Cheong, *Phys. Rev. Lett.* 81 (1998) 3972.
- [6] N.R. Rao, A.K. Cheetham, *Science* 276 (1999) 911.
- [7] Y. Tokura, N. Nagaosa, *Science* 288 (2000) 462.
- [8] P.G. Radaelli, D.E. Cox, M. Marezio, S.-W. Cheong, P.E. Schiffer, A.P. Ramirez, *Phys. Rev. Lett.* 75 (1995) 4488.
- [9] Y. Tomioka, A. Asamita, H. Kuwahara, Y. Moritomo, Y. Tokura, *Phys. Rev. B* 53 (1996) R1689.
- [10] F. Millange, S. de Brion, G. Chouteau, *Phys. Rev. B* 62 (2000) 5619.
- [11] P. Schiffer, A.P. Ramirez, W. Bao, S.W. Cheong, *Phys. Rev. Lett.* 75 (1998) 3336.
- [12] Y. Tomioka, A. Asamitsu, Y. Moritomo, H. Kuwahara, Y. Tokura, *Phys. Rev. Lett.* 74 (1995) 5108.
- [13] M. Tokunaga, N. Miura, Y. Tomioka, Y. Tokura, *Phys. Rev. B* 57 (1998) 5259.
- [14] F. Damay, A. Maignan, C. Martin, B. Raveau, *J. Appl. Phys.* 82 (1997) 1485.
- [15] X. Chen, Z.-H. Wang, R.-W. Li, B.-G. Shen, W.-S. Zhan, J.-R. Sun, J.-S. Chen, C.-H. Yan, *J. Appl. Phys.* 87 (2000) 5594.
- [16] F. Damay, C. Martin, A. Maignan, M. Hervieu, B. Raveau, *Appl. Phys. Lett.* 73 (1998) 3772.
- [17] R. Mahendiran, B. Raveau, M. Hervieu, C. Michel, A. Maignan, *Phys. Rev. B* 64 (2001) 064424.
- [18] T. Kimura, Y. Tomioka, R. Kumai, Y. Okimoto, Y. Tokura, *Phys. Rev. Lett.* 83 (1999) 3940.
- [19] H. Kawano-Furukawa, R. Kajimoto, H. Yoshizawa, Y. Tomioka, H. Kuwahara, Y. Tokura, *Phys. Rev. B* 68 (2003) 174422.
- [20] J. López, P.N. Lisboa-Filho, W.A.C. Passos, W.A. Ortiz, F.M. Araujo-Moreira, O.F. de Lima, D. Schaniel, K. Ghosh, *Phys. Rev. B* 63 (2001) 224422.
- [21] R. Kajimoto, H. Yoshizawa, H. Kawano, H. Kuwahara, Y. Tokura, K. Ohoyama, M. Ohashi, *Phys. Rev. B* 60 (1999) 9506.
- [22] S.B. Oseroff, M. Torikachvili, J. Singley, S. Ali, S.-W. Cheong, S. Schultz, *Phys. Rev. B* 53 (1996) 6521.
- [23] A. Shengelaya, G.-M. Zhao, H. Keller, K.A. Müller, B.I. Kochelaev, *Phys. Rev. B* 61 (2000) 5888.
- [24] A.I. Shames, E. Rozenberg, W.H. McCarroll, M. Greenblatt, G. Gorodetsky, *Phys. Rev. B* 64 (2001) 172401.
- [25] K.A. Mand, C. Benedek, *Phase Separation in Cuprate Superconductor*, World Scientific, Singapore, 1993.
- [26] J. Fan, J. Xie, Y. Ying, L. Pi, Y. Zhang, *Solid State Commun.* 138 (2006) 299.
- [27] E. Houzé, M. Nechtschein, *Phys. Rev. B* 53 (1996) 14309.
- [28] A. Shengelaya, G. Zhao, H. Keller, K.A. Müller, *Phys. Rev. Lett.* 77 (1996) 5296.
- [29] C. Rettori, D. Rao, J. Singley, D. Kidwell, S.B. Oseroff, M.T. Causa, J.J. Neumeier, K.J. McClellan, S.-W. Cheong, S. Schultz, *Phys. Rev. B* 55 (1997) 3083.